J. Biochem. **132**, 205–210 (2002)

A Role of Methionine100 in Facilitating PYP_M-Decay Process in the Photocycle of Photoactive Yellow Protein[1]

Masato Kumauchi, Norio Hamada, Jun Sasaki, and Fumio Tokunaga[2]

Department of Earth and Space Science, Graduate School of Science, Osaka University, Toyonaka, Osaka 560-0043

Received April 16, 2002; accepted May 17, 2002

PYP (photoactive yellow protein) is a photoreceptor protein, which is activated upon photo-isomerization of the *p*-coumaric acid chromophore and is inactivated as the chromophore is thermally back-isomerized within a second (in PYP_M-to-PYP_{dark} conversion). Here we have examined the mechanism of the rapid thermal isomerization by analyzing mutant PYPs of Met100, which was previously shown to play a major role in facilitating the reaction [Devanathan, S. *et al.* (1998) *Biochemistry* 37, 11563–11568]. The mutation to Lys, Leu, Ala, or Glu decelerated the dark state recovery by one to three orders of magnitude. By evaluating temperature-dependence of the kinetics, it was found that the retardation resulted unequivocally from elevations of activation enthalpy ($\Delta H^{\ddagger}$) but not the other parameters such as activation entropy or heat capacity changes. Another effect exerted by the mutations was an up-shift of the apparent pK_a of the chromophore [the pK_a of a titratable group (X) that controls the pK_a of the chromophore] in the PYP_M-decay process. The pK_a up-shift and the $\Delta H^{\ddagger}$ elevation show an approximately linear correlation. We, therefore, postulate that the role of Met100 is to reduce the energy barrier of the PYP_M-decay process by an indirect interaction through X and that the process is thereby facilitated.

Key words: curved temperature dependence of the rate constant, methionine100, Met100-mutant PYP, photoactive yellow protein, PYP_M-decay process.

Photoactive yellow protein (PYP) isolated from *Ectothiorhodospira halophila*, is a 14-kDa, water-soluble protein, consisting of 125 amino acid residues (*1–3*). Its function is believed to be photoreception for negative phototaxis (*4*). For the photoreception, it contains a 4-hydroxycinnamoyl group covalently bound to Cys69 via a thiol-ester as a chromophore (*5, 6*). The phenolic hydroxyl group of the chromophore in PYP in the dark state (PYP_{dark}) is deprotonated (phenolate anion), causing an enormous red-shift of the absorption maximum to 446 nm, and the configuration of the olefinic bond (the C = C bond) is *trans* (*7, 8*). A photocycle of PYP is triggered by light-induced isomerization of the chromophore from *trans* to *cis* configuration (*8, 9*), which initiates subsequent conversions to spectroscopically-distinguishable intermediates before returning to the initial state (*10, 11*). Early intermediates PYP_B (also called I_0, pR_1) (*12–14*) and PYP_L (also called I_1, pR_2) (*15*) whose λ_{max} values are even more red-shifted than that of PYP_{dark} have been shown to have *cis* chromophores with the carbonyl group flipped over and with the other side of the chromophore remaining attached to the protein moiety through the phenolate anion (*16, 17*). Subsequent proton transfer from Glu46 to the phenolic oxygen of the chromophore in the conversion to intermediate PYP_M (also called I_2, pB) (*15, 18, 19*) triggers global conformational changes of the protein moiety (*20, 21*). All these changes that occurred in the course of PYP_M formation are reversed at the end of the photocycle in the PYP_M-to-PYP_{dark} process. The last conversion step is of particular interest from a chemical point of view because it involves a thermal isomerization of olefinic bonds of the chromophore in ~0.5 s (*10, 20*), which is unusual in common solvents at ambient temperature (*22*). In a previous investigation, it was noted that a site-directed mutagenesis of Met100 to Ala (M100A) considerably elevated this barrier, because the PYP_M-decay rate was decelerated by ~1000-fold (*23*). Since the rapid recovery was restored when the olefinic bond of the chromophore was photo-isomerized with a UV-light, it was concluded that the rate-determining step in the PYP_M-decay process was the thermal isomerization, which, in the WT protein, is catalyzed by the Met100 presumably with an electronegative sulfur atom. However, even for the mutant M100A, the *cis* chromophore in PYP_M undergoes thermal isomerization in 1 h, which is still an extraordinarily short time for general thermal isomerization to occur. This evidence argues that there is another catalyst besides Met100 or that a different mechanism for facilitating the thermal isomerization operates in which Ala is partially functional. In an attempt to address these issues, we have constructed site-directed mutant PYPs, M100A, M100L, M100K, and M100E. Each mutant showed a considerably lower but distinct rate constant of PYP_M decay. The decelerations in those mutants were

[1]This work was partly supported by a Grant-in-Aid from the Ministry of Education, Science and Culture of Japan to FT (11304058).

[2]To whom correspondence should be addressed. Tel: +81-6-6850-5499, Fax: +81-6-6850-5542, E-mail: tokunaga@ess.sci.osaka-u.ac.jp

Abbreviations: PYP, photoactive yellow protein; WT, wild-type PYP; M100K, M100E, M100A, and M100L, PYP mutants in which Met100 is replaced with Lys, Glu, Ala, or Leu; PYP_{dark}, PYP in the dark state; $PYP_M^{\ddagger}$, PYP in the activated state in the PYP_M-to-PYP_{dark} conversion; $\Delta C_p^{\ddagger}$, activation isobaric heat capacity; $\Delta H^{\ddagger}$, activation enthalpy; $\Delta S^{\ddagger}$, activation entropy.

ascribed to an elevation of the activation enthalpies ($\Delta H^{\ddagger}$) and the pK_a of PYP_M decay process.

MATERIALS AND METHODS

Plasmid Construction for M100L, M100K, M100A, and M100E and Expression in E. coli—The mutant genes for M100L, M100K, M100A, and M100E were synthesized by PCR using a full-length pyp gene inserted between *Nco*I and *Bam*HI sites of a pET-16b plasmid (*24*) as a template. First, the 5′-half of the DNA fragment of the mutant *pyp* gene was obtained by PCR between a pair of sense and antisense oligonucleotide primers. The sense oligonucleotide primer, GATATACCATGGAACATGTT contains the sequence near the initiation codon with *Nco*I site. The antisense primer was one of the oligonucleotide sequences TCGTGGGCGTCAGTTGGTAATCG, TCGTGGGCGTCTTTTGGTAATCG, and TCGTGGGCGTCGCTTGGTAATCG, TCGTGGGCGTCTCTTGGTAATCG, which contain a sequence of seven amino acids around the mutation site at the 100th position, for M100L, M100K, M100A, and M100E respectively. Likewise the 3′-half of the mutant genes was obtained by PCR using another pair of sense and antisense oligonucleotide primers. The sense primer was one of the oligonucleotide sequences CGATTACCAACTGACGCCCACGA, CGATTACCAAAAGACGCCCACGA, CGATTACCAAGCGACGCCCACGA, and CGATTACCAAGAGACGCCCACGA, which contain a sequence of seven amino acids around the mutation site at the 100th position for M100L, M100K, M100A, and M100E respectively. The antisense primer was the sequence around the stop codon followed by a *Bam*HI site. Full-length genes of the mutants were obtained by PCR using the two sets of DNA fragments both as templates and primers. The mutant gene was amplified as described (*24*) and finally cloned into plasmid vector pET16-b between *Nco*I and *Bam*HI restriction sites. The mutation was confirmed by analyzing the DNA sequence. The expression vector was then transformed into an *Escherichia coli* strain, BL21 (DE3) (*24*). The cells were cultured at 37°C in 2× YT medium containing 50 μg/ml ampicilin. Expression of mutant PYP apoprotein was induced by the addition of isopropyl-thio-β-galactoside (IPTG; final concentration 1 mM) when the optical density at 600 nm of the culture solution reached ~1. After about 4 h, the cells were harvested by centrifugation at 5,000 ×*g* for 15 min (*25*).

Preparation of the WT and the Mutant PYPs—The WT and the mutant holoproteins were reconstituted with *p*-coumaric anhydride as described (*25*). They were then desalted by dialysis and applied to a DEAE-Sepharose CL6B column (Pharmacia Biotech). After washing the applied sample with 10 mM MOPS (3-morpholinopropanesulfonic acid) buffer (pH 7.4), the PYPs were eluted with 100 mM NaCl in the same buffer. This process was repeated until a single band (almost 100% purity) was attained as checked by SDS-PAGE when 10 mg/ml (0.1 mg/lane) sample was loaded and stained with Coomassie Brilliant Blue. Purity indices (A_{278}/A_{446}) of WT, M100K, M100A, M100L, and M100E were 0.43, 0.66, 0.59, 0.56, and 0.45, respectively. The PYPs were then concentrated with an ultrafiltration membrane (Centriprep 10, Amicon) and diluted either with water or 10 mM MOPS buffer. Dilution and concentration steps were repeated several times to remove NaCl.

Determination of Relative Extinction Coefficient of the 4-Hydroxycinnamoyl Chromophore in M100K, M100A, M100L, and M100E—These mutants and WT were denatured in 2% sodium dodecyl sulfate (SDS). The absorption band due to the 4-hydroxycinnamoyl chromophore (~350 nm) in the denatured proteins was used for the normalization.

Measurement of UV-Visible Spectra—UV-visible absorption spectra were recorded at 293 K, in 10 mM MOPS-buffer pH 7.4 by using either U-3210 (Hitachi) or V-550 (JASCO) spectrometer equipped with temperature-controlled sample holder. Accumulation of the PYP_M was performed by illumination with visible light from a 1 kW Xe-lamp (HILUX-HR, Tokyo Master) via a glass optical filter (Y43, Toshiba). The Y43 optical-filter selectively transmits wavelengths longer than 410 nm. All illumination experiments were carried out using the Y43 in order to prevent the photo-reisomerization of PYP_M chromophore (λ_{max} = ~350 nm) by UV irradiation.

RESULTS

Effects of Met100 Mutation on the Absorption Spectra—As described earlier (*23*), the Met100-to-Ala mutant considerably slowed the PYP_M-to-PYP_{dark} process, suggesting a catalytic role of the methionine that facilitates the process. Since the substitution not only eliminated electronic polarity provided by the sulfur atom but reduced the bulkiness, the catalytic role of Met100 can be ascribed to either one of these factors. Thus we have constructed mutant PYPs in which the Met was replaced either with Glu, Lys, Leu, or Ala. All these mutant proteins showed absorption spectra of chromophores with the maxima at 446 nm as in WT (*1*), as shown in Fig. 1 for M100L and M100E. For M100A and M100K, their spectral shapes were almost identical with that of M100L (not shown). Compared to WT, the spectra of M100L, M100K, and M100A show a contribution from a species absorbing near 350 nm beside the red-shifted species absorbing near 446 nm. The blue-shifted species presumably contain a protonated chromophore at the hydroxyl

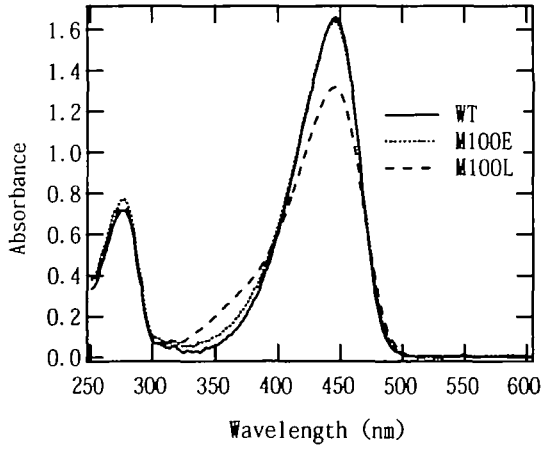

Fig. 1. **Absorption spectra in the visible and near-UV region for WT (solid line), M100E (dotted line), and M100L (dashed line).** The spectral amplitudes were adjusted to represent the same molecular amount of proteins, by adjusting the amplitude of the absorption by the chromophore at 340 nm after denaturating the protein with 2% SDS (data not shown) (to be the same).

group. For M100L, it was shown in our preceding publication (*26*) that the blue-shifted species was thermally in equilibrium with the red-shifted species and that the conversion between them did not involve isomerization of the olefinic bond of the chromophore. Similar analyses were carried out for the other mutants to prove that the protonated species contain exclusively the *trans* chromophore. The above notions point to the fact that the replacement of Met100 somewhat destabilizes the anionic form of the chromophore, although in M100E the equilibrium is shifted more towered the anionic form than the other mutants.

Effects of Met100 Mutations on the Decay Rate of PYP_M— When M100K was illuminated with yellow light (>410 nm) at 293 K, a substantial amount of blue-shifted state with the λ_{max} near 360 nm accumulated (Fig. 2). As in the case of M100A reported earlier (*23*), the recovery of the dark state was slowed by three orders of magnitude. In our preceding paper (*26*), we reported that the corresponding blue-shifted species for M100L was attributed to PYP_M, because the difference IR spectrum between the blue-shifted state and the dark state was almost identical with the PYP_M-PYP_{dark} spectrum of WT. Corresponding difference IR spectra were also recorded for M100K, M100A, and M100E and found to be almost identical with that of WT (Kumauchi, M. and Tokunaga, F., unpublished data), verifying the formation of the same photoproducts for these mutants assignable to PYP_M. Thus, we denote the light-induced blue-shifted species as PYP_M, hereafter.

A rate constant of the PYP_M-PYP_{dark} conversion process for M100K was obtained by fitting the absorbance changes at 356 and 446 nm with a single exponential term (Fig. 2b). The decay rate constant was over 2,000-fold smaller than that of WT. Corresponding kinetic traces for M100L, M100A, and M100E could be also approximated with a single exponential term, respectively (Fig. 3). The PYP_M-decay rate for the mutants with neutral substituents, M100L and M100A, were also reduced by nearly 1,000-fold. On the other hand, PYP_M decay was faster for M100E, though still slower by nearly 20-fold compared to WT. Considering that Glu and Met can provide an electron-donating environment with the carboxylate anion and a lone pair of electrons, respectively, it is suggested that the activation free energy for crossing over the barrier in the PYP_M decay process is

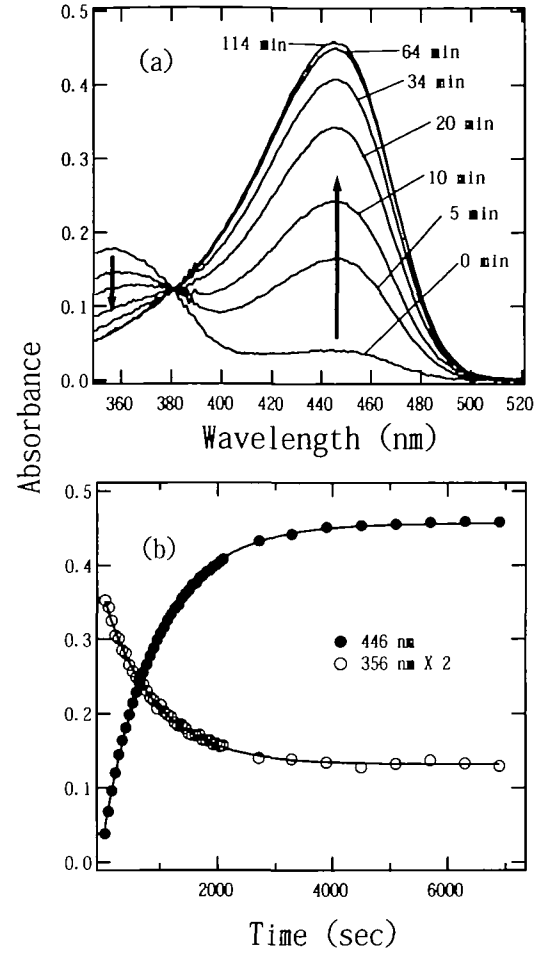

Fig. 2. **(a) Absorption spectra of M100K during the recovery process of PYP_{dark} from PYP_M, following illumination at >410 nm.** Spectral recordings were started immediately after turning off the illumination. Measurements were carried out at 1-min intervals for the first 34 spectra and 10-min intervals for the last 8 spectra. The isobestic point lies at 381 nm. All measurements were carried out in 10 mM MOPS buffer at pH 7.4 at 293 K. **(b) Absorbance changes during the recovery process of PYP_{dark} from PYP_M at 446 nm (λ_{max} of PYP_{dark}, closed circles) and at 356 nm (λ_{max} of PYP_M, open circles).** The changes at the indicated wavelengths represent the recovery of PYP_{dark} and the decay of PYP_M, respectively.

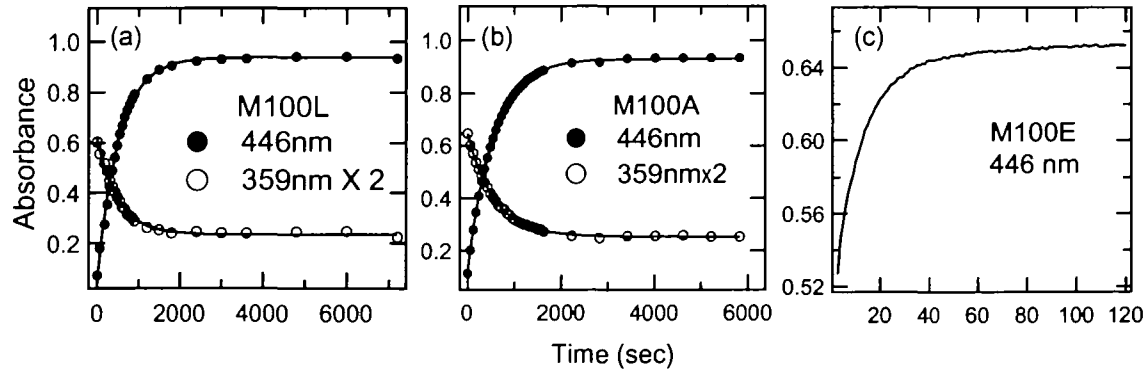

Fig. 3. **Absorbance changes in the PYP_M-to-PYP_{dark} process for M100L, M100A, and M100E.** PYP_M was accumulated by illumination at >410 nm. The spectral measurements were started after turning off the light. Absorbance at 446 nm (closed circles) and near 360 nm (open circles) was plotted as a function of time after turning off the light for M100L (a), and M100A (b). Lines represent single exponential terms fitted to the plots. All measurements were carried out in 10 mM MOPS buffer at pH 7.4 at 293 K. In the case of M100E (c) the kinetic trace at 446 nm was measured by time scan following the illumination.

reduced by the electron-rich environment.

To further examine the factors contributing the reduction of activation free energy, temperature dependences of the PYP_M-decay rate constants for these mutant proteins were analyzed. In Fig. 4, the rate constant of each mutant protein is plotted as a function of reciprocal absolute temperature ($1/T$). All of the mutants showed curvatures in the temperature dependence of the rate constants in the logarithmic representation, showing that the activation enthalpies ($\Delta H^{\ddagger}$) and the activation entropies ($\Delta S^{\ddagger}$) are not constant at these temperatures. Similarly curved temperature dependence of the rate constant for WT has been well documented (27, 28) and is ascribed to the changes of heat capacities ($\Delta C_p^{\ddagger}$) in the activated state ($PYP_M^{\ddagger}$) relative to that of PYP_M, presumably resulted from protein folding conformational changes that occur as $PYP_M^{\ddagger}$ is formed. The temperature dependences of the rate constants (k) were then approximated with Eyring's equation with the heat capacity changes taken into account.

$$\ln k = -\ln (k_B T/h) + \ln K^{\ddagger} \quad (1)$$

$$\ln K^{\ddagger} = -\Delta H^{\ddagger}(T_0)/RT - \Delta C_p^{\ddagger}(1-T_0/T)/R + \Delta S^{\ddagger}(T_0)/R - \Delta C_p^{\ddagger}\ln(T_0/T)/R \quad (2)$$

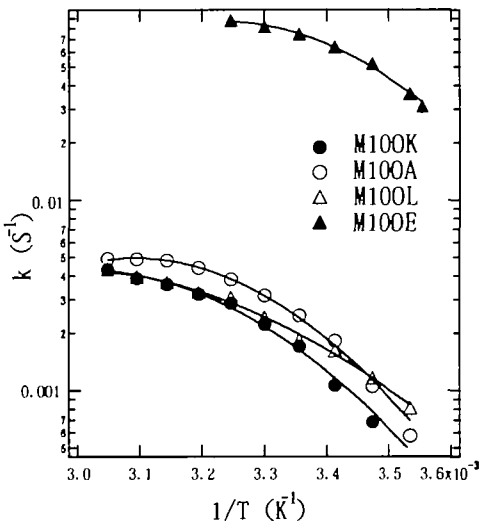

Fig. 4. **Temperature-dependence of the rate constants in the PYP_M-to-PYP_{dark} conversions for M100K (closed circles), M100A (open circles), M100L (open triangles), and M100E (closed triangles).** The rate constant at each temperature was obtained by approximation of each kinetic trace with a single exponential term and was plotted against a reciprocal of the absolute temperature $1/T$ (K^{-1}). Lines represent the equation (II) fitted to the data as described in the text (see "RESULT").

TABLE I. **Activation thermodynamic parameters of PYP_M-to-PYP_{dark} conversion for the Met100-mutant PYPs and the WT (27).** The values in parentheses are the standard deviations.

	$\Delta S^{\ddagger}_{296K}$ (kJ/mol K)	$\Delta H^{\ddagger}_{296K}$ (kJ/mol)	$\Delta C_p^{\ddagger}{}_{296K}$ (kJ/mol K)
WT*	−0.210 (±0.003)	5.5 (±0.9)	−2.81 (±0.1)
M100K	−0.152 (±0.009)	43.6 (±0.05)	−1.42 (±0.18)
M100A	−0.154 (±0.004)	42.1 (±0.02)	−1.76 (±0.09)
M100L	−0.193 (±0.006)	30.9 (±0.03)	−0.86 (±0.12)
M100E	−0.207 (±0.003)	17.6 (±0.02)	−1.78 (±0.23)

*Taken from Ref. 27.

where k_B is Boltzmann's constant, h is Plank's constant, R is the gas constant, and T_0 is any reference temperature. The activation thermodynamic parameters for the mutants as a result of the fits are listed in Table I.

Remarkably, only $\Delta H^{\ddagger}$ was affected by the mutation of Met100, while $\Delta S^{\ddagger}$ and $\Delta C_p^{\ddagger}$ were not significantly perturbed. This means that the deceleration of PYP_M decay for the M100-mutants can be explained solely by the elevation of $\Delta H^{\ddagger}$. In other words, in the wild-type protein, Met100 facilitates the PYP_M decay by reducing the $\Delta H^{\ddagger}$. The increased enthalpy in the activated state ($PYP_M^{\ddagger}$) relative

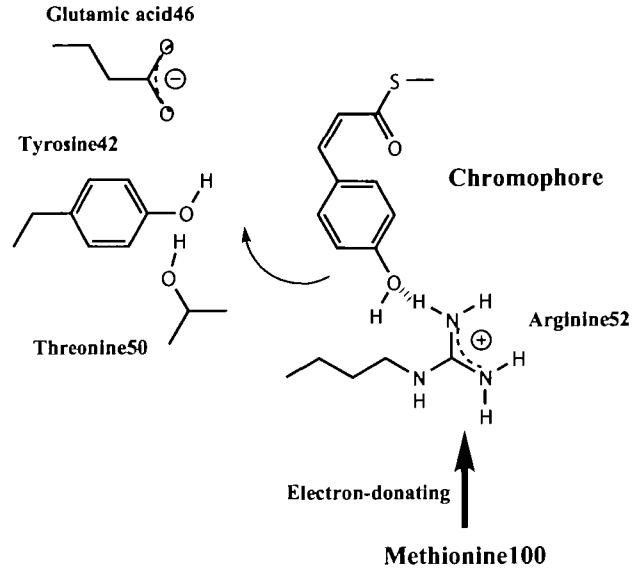

Scheme 1. **Schematic drawing of the molecular mechanism of the action of methionine100.** The scheme was drawn on the basis of X-ray crystallographic study (*16*). In the PYP_M-to-PYP_{dark} conversion, methionine100, as an electron donor, interacts with arginine52.

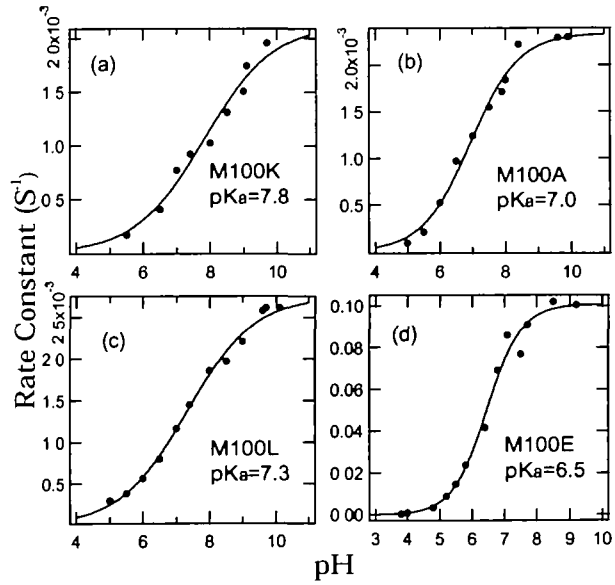

Fig. 5. **The rate constants of the PYP_M-to-PYP_{dark} conversion plotted as a function of pH for M100K (a), M100A (b), M100L (c), and M100E (d).** These plots are approximated with a Henderson-Hasselbalsch equation as shown by the lines.

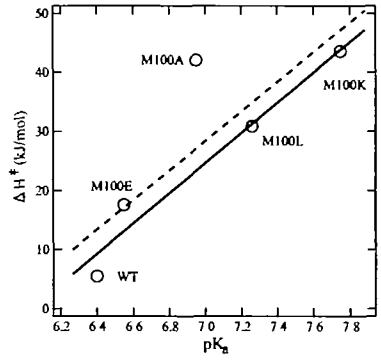

Fig. 6. **Correlation between the activation enthalpies of the PYP_M-decay process and the pK_a.** The dotted line represents the fitted line to the points of WT and all of Met100-mutants. The solid line is the fitted line to the points of WT, M100K, M100L, and M100E.

to the ground state (PYP_M) indicates the involvement of bond cleavage in going from PYP_M to $PYP_M^{\ddagger}$, which must be facilitated by Met100. A similar effect was observed for M100E, though to a lesser degree, indicating that the $\Delta H^{\ddagger}$ was reduced by an electron-donating environment that Met and Glu can provide.

Effects of Met100 Mutations on the pH Dependence of the Rate-Constants of the PYP_M-to-PYP_{dark} Conversions—In the wild-type PYP photocycle, PYP_M decay rate is slowed in the lower pH range (*2*). This pH-dependent behavior of the decay rate can be explained by the presence of a titratable group X (see "DISCUSSION").

Figure 5 shows titration profiles of the rate constants of the PYP_M-decay for the Met100-mutants. These titration profiles were fitted with the Henderson-Hsselbalsch equation to obtain the pK_a of the titratable group X. The pK_a was elevated in the mutants compared to the WT (6.4) (*29*). The pH-rate profile for the WT in Ref. *29* showed a bell-shaped curve with two pK_a values of 6.4 and 9.4. We picked only 6.4, for two reasons: first, we forcused on the accelerated process by base titration; second, we tried to titrate in a higher pH range but reproducible data were not obtained, because the mutants might be more destabilized by base than the WT, and the resulting curves were not bell-shaped. The values obtained were 7.0, 7.3, 7.8, and 6.5, for M100A, M100L, M100K, and M100E, respectively. As in the case of $\Delta H^{\ddagger}$ elevation, the Glu-mutant showed a greater elevation of the pK_a than the other mutants. It is, therefore, likely that X is regulated through the electron-rich environment, which Met and, to a lesser extent, Glu can provide.

Correlation Between the $\Delta H^{\ddagger}$ and the pK_a—Since $\Delta H^{\ddagger}$ is negatively proportional to the natural logarithm of the activation equilibrium constant ($\ln K^{\ddagger} \propto -\Delta H^{\ddagger} + T\Delta S^{\ddagger}$) when $\Delta S^{\ddagger}$ and $\Delta C_p^{\ddagger}$ are constant, it follows that $\ln K^{\ddagger}$ is correlated with the pK of the group X. Also, $K^{\ddagger}$ is proportional to k (PYP_M-decay rate constant). In Fig. 6, the $\Delta H^{\ddagger}$ of each Met100 mutant is plotted versus the pK_a of X determined in the PYP_M-decay process. $\Delta H^{\ddagger}$ and pK_a show approximately a linear correlation. This means that the ratio of $PYP_M^{\ddagger}$ increases with increasing K (decreasing pK), resulting in an increase in the rate of the PYP_M -decay process.

DISCUSSION

Mutations of Met100 either to a positively or a negatively chargeable residue, Lys or Glu, or to a neutral residue of different size, Leu or Ala, were shown in the present paper to display extraordinarily slowed rates for the conversion from PYP_M to PYP_{dark} as compared with the WT. The effect was mainly ascribed to an increase in $\Delta H^{\ddagger}$ in the PYP_M-decay process for these mutants rather than to other activation thermodynamic parameters, such as $\Delta S^{\ddagger}$ or $\Delta C_p^{\ddagger}$. This indicates that Met100 affects the PYP_M-decay process, which involves heat absorption due to a cleavage or formation of chemical bonds in the conversion to the activation state ($PYP_M^{\ddagger}$).

In the Glu-mutant, which has a negative charge or a lone pair of electrons, the elevating effect of $\Delta H^{\ddagger}$ (and thus the decay rate deceleration) was moderate compared to the other mutants. On the other hand, in the Lys-mutant, which has a positive charge, the $\Delta H^{\ddagger}$ was elevated the most of all these mutants; and in the Ala- and Leu-mutants which have a neutral side-chain, $\Delta H^{\ddagger}$ values were intermediate between those of the Glu-mutant and the Lys-mutant. This suggests that the electron-donating character at 100th position plays a role of facilitating the heat-absorbing process. The lack of electron-donating character results in the PYP_M decay rate deceleration. In Fig. 6, $\Delta H^{\ddagger}$ of the Ala-mutant deviates from the fitted line (dotted-line), possibily not only because of the lack of Met100 but also due to another factor. We consider that the Ala-mutant is the exception among the PYPs, because the fitted line, except for the Ala-mutant (solid-line), shows a linear relationship between $\Delta H^{\ddagger}$ and pK_a. One possible reason for the deviation in the Ala-mutant is that Ala has a smaller side-chain than the other substituents, and therefore the local structure near the 100th position may be effectively different from that of the WT and other mutants. In addition, a previous report (*29*) showed that Ala-mutant PYP (R52A) demonstrated a strong influence of specific interactions in the active-site chemical environment. This may result in the abnormal behavior of the Ala-mutant in the PYP_M-decay process.

Another finding was that these mutations affected the pK_a of the PYP_M decay rate constant (pK_a of X). The pH dependence of the rate constant of PYP_M-decay as shown in Fig. 5 can be accounted for by the presence of a titratable group (X) that controls the PYP_M-decay process. X is not the pCA chromophore but another residue(s), because the intrinsic pK_a of the pCA thiol-ester in solution is ~9 (*30*). Therefore, in the PYP_M-decay process, the pCA chromophore is insulated from the outer environment and is not titrated directly. Also, X should be located near both Met100 and the chromophore, because it interacts with both Met100 and the chromophore. In the previous report (*16*), Arg52 interacted with the chromophore and is located near Met100 in the PYP_M. We suggest, therefore, that X may be Arg52 (Scheme). Met100 interacts, as an electron-donor, with Arg52 in the PYP_M-to-PYP_{dark} conversion. The electron-donation from Met100 may weaken the interaction between the chromophore and Arg52, allowing the chromophore could change its conformation toward to the PYP_{dark}. Met100 controls the pK_a of Arg52 by providing the electron-donating environment, and then the energy bar-

rier in this process is reduced. Thus Met100 facilitates the thermal process in the PYP_M-to-PYP_{dark} conversion.

REFERENCES

1. Meyer, T.E. (1985) Isolation and characterization of soluble cytochromes, ferredoxins and other chromophoric proteins from the halophilic phototrophic bacterium *Ectothiorhodospira halophila*. *Biochim. Biophys. Acta* **806**, 175–183
2. Meyer, T.E., Yakali, E., Cusanovich, M.A., and Tollin, G. (1987) Properties of a water-soluble, yellow protein isolated from a halophilic phototrophic bacterium that has photochemical activity analogous to sensory rhodopsin. *Biochemistry* **26**, 418–423
3. Van Beeumen, J.J., Devreese, B.V., Van Bun, S.M., Hoff, W.D., Hellingwerf, K.J., Meyer, T.E., McRee, D.E., and Cusanovich, M.A. (1993) Primary structure of a photoactive yellow protein from the phototrophic bacterium *Ectothiorhodospira halophila*, with evidence for the mass and the binding site of the chromophore. *Protein Sci.* **2**, 1114–1125
4. Sprenger, W.W., Hoff, W.D., Armitage, J.P., and Hellingwerf, K.J. (1993) The eubacterium *Ectothiorhodospira halophila* is negatively phototactic, with a wavelength dependence that fits the absorption spectrum of the photoactive yellow protein. *J. Bacteriol.* **175**, 3096–3104
5. Hoff, W.D., Dux, P., Hard, K., Devreese, B., Nugteren-Roodzant, I.M., Crielaard, W., Boelens, R., Kaptein, R., van Beeumen, J., and Hellingwerf, K.J. (1994) Thiol ester-linked *p*-coumaric acid as a new photoactive prosthetic group in a protein with rhodopsin-like photochemistry. *Biochemistry* **33**, 13959–13962
6. Hoff, W.D., Devreese, B., Fokkens, R., Nugteren-Roodzant, I.M., Van Beeumen, J., Nibbering, N., and Hellingwerf, K.J. (1996) Chemical reactivity and spectroscopy of the thiol ester-linked *p*-coumaric acid chromophore in the photoactive yellow protein from Ectothiorhodospira halophila. *Biochemistry* **35**, 1274–1281
7. Kim, M., Mathies, R.A., Hoff, W.D., and Hellingwerf, K.J. (1995) Resonance Raman evidence that the thioester-linked 4-hydroxycinnamyl chromophore of photoactive yellow protein is deprotonated. Biochemistry **34**, 12669–12672
8. Unno, M., Kumauchi, M Sasaki, J., Tokunaga, F., and Yamauchi, S. (2000) Evidence for a protonated and *cis* configuration chromophore in the photobleached intermediate of photoactive yellow protein. *J. Am. Chem. Soc.* **122**, 4233–4234
9. Kort, R., Vonk, H., Xu, X., Hoff, W.D., Crielaard, W., and Hellingwerf, K.J. (1996) Evidence for trans-cis isomerization of the *p*-coumaric acid chromophore as the photochemical basis of the photocycle of photoactive yellow protein. *FEBS Lett.* **382**, 73–78
10. Meyer, T.E., Tollin, G., Hazzard, J.H., and Cusanovich, M.A. (1989) Photoactive yellow protein from the purple phototrophic bacterium, *Ectothiorhodospira halophila*. Quantum yield of photobleaching and effects of temperature, alcohols, glycerol, and sucrose on kinetics of photobleaching and recovery. *Biophys. J.* **56**, 559–564
11. Hoff, W.D., van Stokkum, I.H., van Ramesdonk, H.J., van Brederode, M.E., Brouwer, A.M., Fitch, J.C., Meyer, T.E., van Grondelle, R., and Hellingwerf, K.J. (1994) Measurernent and global analysis of the absorbance changes in the photocycle of the photoactive yellow protein from *Ectothiorhodospira halophila*. *Biophys. J.* **67**, 1691–1705
12. Ujj, L., Devanathan, S., Meyer, T.E., Cusanovich, M.A., Tollin, G., and Atkinson, G.H. (1998) New photocycle intermediates in the photoactive yellow protein from *Ectothiorhodospira halophila*: picosecond transient absorption spectroscopy. *Biophys. J.* **75**, 406–412
13. Devanathan, S., Pacheco, A., Ujj, L., Cusanovich, M., Tollin, G., Lin, S., and Woodbury, N. (1999) Femtosecond spectroscopic observations of initial intermediates in the photocycle of the photoactive yellow protein from *Ectothiorhodospira halophila*. *Biophys. J.* **77**, 1017–1023
14. Imamoto, Y., Kataoka, M., Tokunaga, F., Asahi, T., and Masuhara, H. (2001) Primary photoreaction of photoactive yellow protein studied by subpicosecond-nanosecond spectroscopy. *Biochemistry* **40**, 6047–6052
15. Meyer, T.E., Cusanovich, M.A., and Tollin, G. (1993) Transient proton uptake and release is associated with the photocycle of the photoactive yellow protein from the purple phototrophic bacterium *Ectothiorhodospira halophila*. *Arch. Biochem. Biophys.* **306**, 515–517
16. Genick, U.K., Borgstahl, G.E., Ng, K., Ren, Z., Pradervand, C., Burke, P.M., Srajer, V., Teng, T.Y., Schildkamp, W., McRee, D.E., Moffat, K., and Getzoff, E.D. (1997) Structure of a protein photocycle intermediate by millisecond time-resolved crystallography. *Science* **275**, 1471–1475
17. Brudler, R., Rammelsberg, R., Woo, T.T., Getzoff, E.D., and Gerwert, K. (2001) Structure of the I1 early intermediate of photoactive yellow protein by FTIR spectroscopy. *Nat. Struct. Biol.* **8**, 265–270
18. Xie, A., Hoff, W.D., Kroon, A.R., and Hellingwerf, K.J. (1996) Glu46 donates a proton to the 4-hydroxycinnamate anion chromophore during the photocycle of photoactive yellow protein. *Biochemistry* **35**, 14671–14678
19. Imamoto, Y., Mihara, K., Hisatomi, O., Kataoka, M., Tokunaga, F., Bojkova, N., and Yoshihara, K. (1997) Evidence for proton transfer from Glu-46 to the chromophore during the photocycle of photoactive yellow protein. *J. Biol. Chem.* **272**, 12905–12908
20. Hoff, W.D., Xie, A., Van Stokkum, I.H., Tang, X.J., Gural, J., Kroon, A.R., and Hellingwerf, K.J. (1999) Global conformational changes upon receptor stimulation in photoactive yellow protein. *Biochemistry* **38**, 1009–1017
21. Lee, B.C., Croonquist, P.A., Sosnick, T.R., and Hoff, W.D. (2001) PAS domain receptor photoactive yellow protein is converted to a molten globule state upon activation. *J. Biol. Chem.* **276**, 20821–20823
22. Bastianelli, C., Caia, C., Cum, G., Gallo, R., and Mancini, V. (1991) Thermal isomerization of photochemmically synthesized (*Z*)-9-styrylacridines. An unusually high entropy of Z → E conversion for stilbene-like compounds. *J. Chem. Soc. Perkin Trans.* **2**, 679–683
23. Devanathan, S., Genick, U.K., Canestrelli, I.L., Meyer, T.E., Cusanovich, M.A., Getzoff, E.D., and Tollin, G. (1998) New insights into the photocycle of *Ectothiorhodospira halophila* photoactive yellow protein: photorecovery of the long-lived photobleached intermediate in the Met100Ala mutant *Biochemistry* **37**, 11563–11568
24. Mihara, K., Hisatomi, O., Imamoto, Y., Kataoka, M., and Tokunaga, F. (1997) Functional expression and site-directed mutagenesis of photoactive yellow protein. *J. Biochem.* **121**, 876–880
25. Imamoto, Y., Ito, T., Kataoka, M., and Tokunaga, F. (1995) Reconstitution photoactive yellow protein from apoprotein and *p*-coumaric acid derivatives. *FEBS Lett.* **374**, 157–160
26. Sasaki, J., Kumauchi, M., Hamada, N., Oka, T., and Tokunaga, F. (2002) Light-induced unfolding of photoactive yellow protein mutant M100L. *Biochemistry* **41**, 1915–1922
27. Van Brederode, M.E., Hoff, W.D., Van Stokkum, I.H., Groot, M.L., and Hellingwerf, K.J. (1996) protein folding thermodynamics applied to the photocycle of the photoactive yellow protein. *Biophys. J.* **71**, 365–380
28. van der Horst, M.A., van Stokkum, I.H., Crielaard, W., and Hellingwerf, K.J. (2001) The role of the N-terminal domain of photoactive yellow protein in the transient partial unfolding during signalling state formation. *FEBS Lett.* **497**, 26–30
29. Genick, U.K., Devanathan, S., Meyer, T.E., Canestrelli, I.L., Williams, E., Cusanovich, M.A., Tollin, G., and Getzoff, E.D (1997) Active site mutants implicate key residues for control of color and light cycle kinetics of photoactive yellow protein. *Biochemistry* **36**, 8–14
30. Kroon, A.R., Hoff, W.D., Fenneman, H.P.M., Gijzen, J., Koomen, G.J., Verhoeven, J.W., Crielaard, W., and Hellingwerf, K.J. (1996) Spectral tuning, fluorescence, and photoactivity in hybrinds of photoactive yellow protein, reconstituted with native or modified chromophores. *J. Biol. Chem.* **271** 31949–31956